Multiple phase-coherent laser pulses in optical spectroscopy. II. Applications to multilevel systems

W. S. Warren and Ahmed H. Zewail

Citation: The Journal of Chemical Physics **78**, 2298 (1983); doi: 10.1063/1.445084
View online: http://dx.doi.org/10.1063/1.445084
View Table of Contents: http://scitation.aip.org/content/aip/journal/jcp/78/5?ver=pdfcov
Published by the AIP Publishing

Multiple phase-coherent laser pulses in optical spectroscopy. II. Applications to multilevel systems

W. S. Warren[a] and Ahmed H. Zewail[b]

Arthur Amos Noyes Laboratory of Chemical Physics,[c] California Institute of Technology, Pasadena, California 91125

(Received 28 July 1982; accepted 4 November 1982)

The effects of intense laser pulse trains in coupled multilevel systems (such as pure or mixed molecular crystals) are analyzed by calculating exact density matrix evolutions. It is shown that two-level approximations are inadequate. The contributions of exchange couplings, inhomogeneous broadening, permanent multipole interactions and transition multipole interactions to absorption and photon echo line shapes are calculated. The absorption line shape of 1,4-dibromonaphthalene (DBN) is shown to be predominantly an isotopic substitution effect, as our Monte Carlo results give quantitative agreement with experiment for this model. Average t-matrix approximations to the Green's function, which have been used to propose a different mechanism for the DBN line shape are shown to be qualitatively inadequate. Dipole–dipole interactions are shown to be an important photon echo decay mechanism in mixed crystals, with the relative importance of permanent and transition multipole interactions dependent on the resonance frequency distribution. Multiple pulse trains, including multiple pulse echoes and optical multiple-quantum sequences, are shown to be capable of distinguishing different types of interactions in the molecular Hamiltonian and reducing optical density effects. Specific pulse sequences are proposed and their effects are calculated.

I. INTRODUCTION

For many optical systems the generalized two-level perspective of the preceding paper (including open systems, coupling to a bath and inhomogeneous distributions) is insufficient to describe coherent effects, and an explicitly multilevel approach must be taken. For example, the density of states of even isolated molecules is often high enough that a single laser pulse can coherently excite many distinct transitions. This can lead to such effects as quantum beats in the resolved fluorescence of large molecules.[1–3] Any description of these phenomena must involve at least two excited states and one ground state, and complex beat patterns require a larger set. The situation is even more complicated in condensed phases, where each molecule is often coupled to many others, and the number of contributing energy levels can be incredibly large.

In this paper we will discuss the effects of multiple pulse trains on N level systems, where N is absolutely unrestricted. The density matrix of such a system can, of course, be astronomically large, yet by remaining in this operator formalism we can still derive explicit line shapes, effects of different interactions, and useful pulse sequences. While this may seem surprising to the uninitiated, the power of this formalism has been known to NMR spectroscopists for many years. In fact, many of our results are analogous to theirs, but optical spectroscopy shows some important and interesting differences. Multiple-pulse sequences can be designed to separate the effects of different electronic interactions and to overcome the complications introduced by radiative spontaneous emission. This paper will address the application of these sequences to characterize large systems, particularly solids, which must be viewed from a multilevel perspective.

II. DEPHASING IN OPTICAL MULTILEVEL SYSTEMS

A. The multilevel Hamiltonian

Consider a set of N identical molecules and assume that each of these molecules has one allowed electronic transition from its ground state G to its excited state E. If the molecules were noninteracting, then this set could be treated as an ensemble of two-level systems or as a single system with 2^N levels [Fig. 1(a)]. The two-level approach is of course mathematically simpler and entirely equivalent to the multilevel approach in this limit.

In real condensed phases, however, the molecules will interact in many different ways, splitting the energy levels as in Fig. 1(b). For example, if molecule i is excited and a nearby molecule j is not, overlap of the electronic wave functions at the two sites (exchange mechanism) will generally give the excitation some probability of changing sites. This corresponds to an interaction of the form

$$\mathcal{H}_{ex} = V_{ij}(\sigma_i^+ \sigma_j^- + \sigma_i^- \sigma_j^+) , \tag{1}$$

where σ^+ and σ^- are the usual raising and lowering operators:

$$\sigma^+ = \sigma_x + i\sigma_y , \tag{2}$$

$$\sigma^- = \sigma_x - i\sigma_y , \tag{3}$$

where σ_x, σ_y, and σ_z are the Pauli matrices in the site representation, and V_{ij} is the coupling matrix element between sites. Substituting Eqs. (2) and (3) into Eq. (1) gives

[a] National Science Foundation Postdoctoral Fellow, 1981. Present address: Department of Chemistry, Princeton University, Princeton, New Jersey 08544.

[b] Alfred P. Sloan Fellow and Camille & Henry Dreyfus Foundation Teacher-Scholar.

[c] Contribution No. 6662.

 0021-9606/83/052298-14$2.10

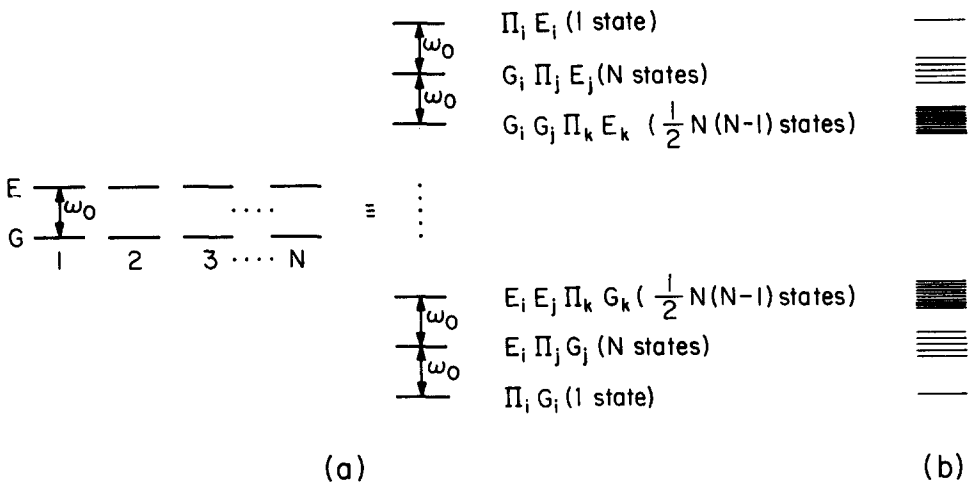

FIG. 1. Energy level diagram for N two-level systems in the absence of couplings [part (a)] and in the presence of couplings [part (b)]. The uncoupled systems can be handled quite well from a two-level perspective. The coupled system has nondegenerate energy levels and all 2^N levels must generally be considered.

$$\mathcal{H}_{ex} = 2V_{ij}(\sigma_{xi}\sigma_{xj} + \sigma_{yi}\sigma_{yj}) \ . \tag{4}$$

Even if the two wave functions do not substantially overlap, interactions between the electronic charge distributions on the two sites will generate a term in the Hamiltonian with this same form. The coefficient of the operator $\sigma_i^+\sigma_j^-$, e.g., is

$$\int \psi_{E_i}^* \psi_{G_j}^* \frac{e(\tau_i)\, e(\tau_j)}{|\tau_i - \tau_j|} \psi_{G_i} \psi_{E_j} \, d\tau_i \, d\tau_j \ , \tag{5}$$

where τ_i and τ_j are the two molecular coordinates, with $e(\tau_i)$ and $e(\tau_j)$ the electronic charge distributions. This can of course be expanded in transition multipole moments, the first term being

$$(\mu^2/r_{ij}^3)[\cos(\theta_i - \theta_j) - 3\cos\theta_i \cos\theta_j] \ , \tag{6}$$

where θ_i and θ_j are the angles between the dipoles and the intermolecular axis, and μ is the transition dipole moment.

We will neglect all matrix elements between states with different numbers of excited sites, since such matrix elements probably involve a large energy mismatch. Actually, this neglect follows immediately from the rotating wave approximation discussed in paper I. In the rotating frame such matrix elements oscillate rapidly and are expected to be unimportant.

In a localized excitation basis set (involving only states such as $G_1 E_2 G_3$ or $E_1 G_2 E_3$ in which the ith molecule is either definitely excited or definitely not excited) terms such as $\mathcal{H}_{ex}$ are exclusively off-diagonal. Diagonal terms come from many different sources, such as:

(1) Crystal strains or isotopic substitutions may make the electronic transition frequency site dependent, introducing a term such as

$$\mathcal{H}_{in} = \sum_i \omega_i \sigma_{zi} \ . \tag{7}$$

This corresponds exactly to inhomogeneous broadening in two-level systems.

(2) Exciting one site of a molecule may change the local structure of the crystal dramatically, thus changing the resonance frequencies of other sites. This means, e.g., that an observed excitation energy of $\hbar\omega_1$ for molecule 1 and $\hbar\omega_2$ for molecule 2 need not imply that the doubly excited state has energy $\hbar(\omega_1 + \omega_2)$. For simplicity we will assume that these effects can be written entirely in terms of two-site interactions, i.e.,

$$\mathcal{H}_{loc} = A_{ij}\sigma_{zi}\sigma_{zj} \ . \tag{8}$$

(3) Permanent multipole interactions must also be included. For example, suppose there are only three sites (with negligible wave function overlap) and the stabilization energy of the state $E_1 G_2 E_3$ is desired. This energy will be

$$\int \psi_{E1}^* \psi_{G2}^* \psi_{E3}^* \left[\frac{e(\tau_1)\, e(\tau_2)}{|\tau_1 - \tau_2|} + \frac{e(\tau_1)\, e(\tau_3)}{|\tau_1 - \tau_3|} + \frac{e(\tau_2)\, e(\tau_3)}{|\tau_2 - \tau_3|}\right] \times \psi_{E1}\psi_{G2}\psi_{E3} \, d\tau_1 \, d\tau_2 \, d\tau_3 \ . \tag{9}$$

If the molecules are electrically neutral, the lowest order approximation to Eq. (9) is to calculate the interaction energy of the static dipoles of the ground state on sites 1 and 3 and the excited state on site 2.

Fortunately Eq. (9) involves only pairs of sites, so the operators it introduces into the Hamiltonian can be written as

$$\mathcal{H}_{dip} = \sum_{i,j} A + B\sigma_{zi} + C\sigma_{zj} + D\sigma_{zi}\sigma_{zj} \ , \tag{10}$$

where the coefficients A, B, C, and D can be evaluated if the energies of the different combinations of excited and ground state dipoles are known.

We can include all of the effects discussed above by writing the system general Hamiltonian (in the rotating wave approximation) as

$$\mathcal{H} = \overline{\Delta\omega}\sigma_z + \sum_i \Delta\omega_i\sigma_i + \sum_{i>j} Q_{ij}\sigma_{zi}\sigma_{zj} - \sum_{i>j} 2V_{ij}(\sigma_{xi}\sigma_{xj} - \sigma_i \cdot \sigma_j) \ , \tag{11}$$

$$= \overline{\Delta\omega}\sigma_z + \sum \Delta\omega_i\sigma_i + \sum_{i>j} J_{ij}\sigma_i \cdot \sigma_j + \sum D_{ij}(3\sigma_{zi}\sigma_{zj} - \sigma_i \cdot \sigma_j) \ , \tag{12}$$

$$D_{ij} = \tfrac{1}{3}(Q_{ij} - 2V_{ij}); \quad J_{ij} = \tfrac{1}{3}(Q_{ij} + 4V_{ij}). \tag{13}$$

Expression (11) reminds us of the physical difference[4]

between the diagonal and off-diagonal terms and as we shall show is convenient for describing photon echoes. Equation (12) is precisely the NMR Hamiltonian for spins in a solid[5] or anisotropic liquid,[6,7] and this will permit a vast number of NMR results to be transferred almost directly to optical spectroscopy. It is also a convenient way to write the Hamiltonian when analyzing the effects of multiple-pulse sequences, as will be seen in Sec. III, because the last three terms all correspond to different irreducible tensors.

Just as with two-level systems, the effect of a laser pulse in the rotating wave approximation is to add another term of the form $\omega_1(\sigma_x \cos\varphi + \sigma_y \sin\varphi)$ to the Hamiltonian.

B. Density matrix evolution

One tremendous advantage of the density matrix-rotation operator approach of paper I is that it is readily extended to multilevel systems. A time independent Hamiltonian still generates a unitary transformation with the propagator $U = \exp(-i\mathcal{H}t)$. If ω_1 is large enough, then the Hamiltonian in Eq. (11) can be neglected during any pulse, so pulses still generate simple rotations such as $\exp[-i(\pi/2)\sigma_x]$. The two major additional complications come from the form of the equilibrium Hamiltonian and the time evolution in the absence of pulses.

The first of these differences is readily calculated. Statistical mechanics still predicts the equilibrium density matrix. In NMR ρ_{eq} still has the form $\rho_{eq} = \exp(-\beta\mathcal{H})/\mathrm{Tr}[\exp(-\beta\mathcal{H})]$, with $\beta \ll 1$ and $I_z = \sum I_{zi}$; every state is populated almost equally. In the low temperature limit of optical spectroscopy every molecule is in the ground state:

$$\rho_{eq} = \begin{pmatrix} 0 & 0 & 0 & \bullet & \bullet & \bullet & 0 \\ 0 & 0 & 0 & \bullet & \bullet & \bullet & 0 \\ 0 & 0 & 0 & \bullet & \bullet & \bullet & 0 \\ \bullet & \bullet & \bullet & \bullet & \bullet & \bullet & \bullet \\ \bullet & \bullet & \bullet & \bullet & \bullet & \bullet & \bullet \\ \bullet & \bullet & \bullet & \bullet & \bullet & \bullet & \bullet \\ 0 & 0 & 0 & \bullet & \bullet & \bullet & 1 \end{pmatrix} .$$

An alternative to the single site Pauli matrices $\mathbf{1}_i$, σ_{xi}, σ_{yi}, σ_{zi} as a basis set is

$$\sigma_G = \begin{pmatrix} 0 & 0 \\ 0 & 1 \end{pmatrix}, \quad \sigma_E = \begin{pmatrix} 1 & 0 \\ 0 & 0 \end{pmatrix},$$

$$\sigma_+ = \begin{pmatrix} 0 & 1 \\ 0 & 0 \end{pmatrix}, \quad \sigma_- = \begin{pmatrix} 0 & 0 \\ 1 & 0 \end{pmatrix}, \tag{14}$$

which we shall call the single element basis. In this basis set

$$\rho_{eq} = \sigma_{G1}\ \sigma_{G2}\ \cdots\ \sigma_{GN} = \prod_i \sigma_{Gi}\ , \tag{15}$$

which is certainly simpler than the equivalent expression

$$\rho_{eq} = \prod_i (1_i - \sigma_{zi})$$

$$= 1 - \sigma_z + \sum_{i,j} \sigma_{zi}\sigma_{zj} - \sum_{i,j,k} \sigma_{zi}\sigma_{zj}\sigma_{zk} + \cdots\ . \tag{16}$$

In addition, while the $(2^N \times 2^N)$ matrix representation of an N site Pauli operator (such as $\sigma_{x1}\mathbf{1}_2\sigma_{z3}\cdots\sigma_{yN}$) has 2^N nonvanishing elements (two for each site), the matrix representation of an N site single element operator has 1^N (one) nonvanishing element, as in Eq. (15). Generally, however, the Pauli matrices are more convenient for calculations. We will use these basis sets interchangeably in the rest of this paper.

The second major difference is that the Hamiltonian in Eq. (11) generates very complicated rotations. In a two-level system rotations always take σ_x (e.g.) to σ_x, σ_y, or σ_z, so that the entire time evolution can be viewed in a three dimensional space. But if one starts with $\sigma_x = \sum_i \sigma_{xi}$ in a multilevel system many other operators creep in rapidly. For example, suppose $\rho(t)$ contains σ_x as one of its operators. Then $\dot{\rho}(t) = -i[\mathcal{H}, \rho(t)]$ will contain

$$-i[\mathcal{H}, \sigma_x] = \Delta\omega\sigma_y - \sum \omega_i \sigma_{yi}$$

$$+ \sum D_{ij}(3\sigma_{yi}\sigma_{zj} + 3\sigma_{zi}\sigma_{yj})\ . \tag{17}$$

The next derivative $\ddot{\rho}(\tau)$ is given by $-i[\mathcal{H}, \dot{\rho}(t)]$, so it will contain operators such as $\sigma_{yi}\sigma_{xj}\sigma_{xk}$. If $\|\mathcal{H}\tau\| \geq 1$ then the Taylor expansion will converge very slowly, high-order derivatives will become important, and many operators will have to be included.

These additional multisite operators complicate the observable spectrum tremendously. They arise solely because of the bilinear operators in the J and D (or Q and V) couplings; if only the linear operators $\omega_i\sigma_{zi}$ are present, the commutators in Eq. (17) only produce the linear operators σ_{xi}, σ_{yi}, and σ_{zi}. Each inequivalent site then acts like an isolated two-level system. The couplings give a more complicated spectrum, but in compensation if they can be measured they give much physical insight into the nature of solid state interactions. The objective of the next two chapters is to show how these couplings affect simple experiments, and to derive multiple-pulse sequences which will help to extract useful information.

III. SIMPLE PULSE SEQUENCES IN MULTILEVEL SYSTEMS

A. Single pulse experiments and absorption measurements

Suppose that a single pulse with $\omega_1 \gg \Delta\omega_i$, J_{ij}, and D_{ij}, and flip angle $\theta = \omega_1 t_p$ is applied to a system of N molecules at equilibrium. The resultant density matrix is then

$$\rho(t_p^+) = \exp[-i(\theta\sigma_x + \overline{\Delta\omega}\, t_p\sigma_z)]$$
$$\times \rho_{eq} \exp[i(\theta\sigma_x + \overline{\Delta\omega}\, t_p\sigma_z)]\ . \tag{18}$$

The free induction decay after a time τ is given by

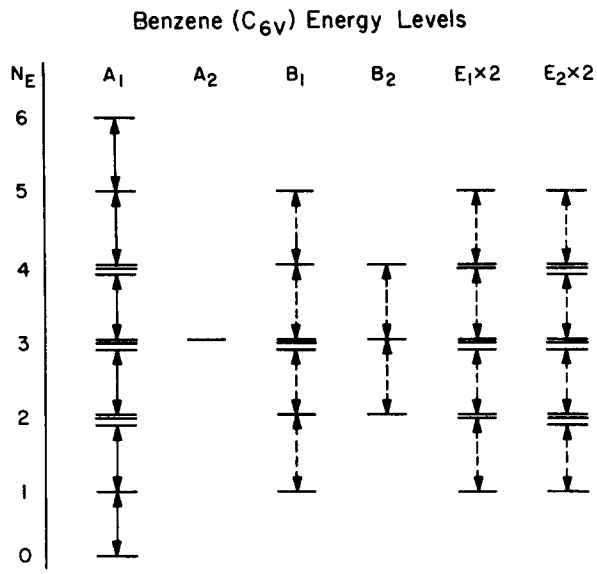

FIG. 2. Energy level diagram for a set of six coupled two-level systems with C_{6v} or D_{6h} symmetry (e.g., the proton NMR of benzene in an orienting solvent). In the optical case all molecules would start in the total system ground state ($N_E=0$), and only the transitions with solid arrows are allowed. In the NMR case the excited states have a nonnegligible equilibrium population and the dotted transitions are also observed. Thus symmetry restrictions will make these two cases different, even though the mathematical analogy is fairly strong.

$$\langle\sigma_x(\tau)\rangle = \mathrm{Tr}[\sigma_x \exp(-i\mathcal{H}\tau)\rho(t_p)\exp(i\mathcal{H}\tau)]\,, \tag{19}$$

$$= \sum_{i,j} \langle i|\sigma_x|j\rangle\langle j|\rho(t_p)|i\rangle \exp[i(E_i-E_j)\tau/\hbar]\,, \tag{20}$$

$$\langle\sigma_y(\tau)\rangle = \mathrm{Tr}[\sigma_y \exp(-i\mathcal{H}\tau)\rho(t_p)\exp(i\mathcal{H}\tau)]\,, \tag{21}$$

$$= \sum_{i,j} \langle i|\sigma_y|j\rangle\langle j|\rho(t_p)|i\rangle \exp[i(E_i-E_j)\tau/\hbar]\,, \tag{22}$$

where i and j are eigenstates of $\mathcal{H}$ with energies E_i and E_j, respectively. We are of course assuming in Eqs. (19)–(22) that phase sensitive detection is used, which requires one more pulse in the optical case as discussed earlier.[8] Since σ_x and σ_y have nonzero matrix elements only for transitions involving exactly one molecule changing from E to G, or G to E, only these single-quantum transitions will be observed.

These expressions are valid in either NMR or optical spectroscopy; the major differences between the NMR spectra of molecules in anisotropic solvents [which generally have the Hamiltonian of Eq. (12)] and the optical spectra of low temperature solids come from differences in ρ_{eq}. For example, there are different symmetry selection rules. Assume that the Hamiltonian in Eq. (12) has benzenelike (D_{6h}) symmetry for some set of six molecules. The $2^6=64$ eigenstates can then be grouped into the irreducible representations of Fig. 2.[9] The initial state of an optical system ($\Pi_i \sigma_{Gi}$) clearly has A_1 symmetry, and there are no symmetry violating terms in $\mathcal{H}$, so only the A_1 single-quantum transitions can be observed (solid lines). This restriction is a consequence of the low temperature form of ρ_{eq}. In the high temperature (NMR) limit all the eigenstates are initially populated, so other transitions are also allowed (dotted lines) as in NMR.

The form of ρ_{eq} also affects the relative intensities of the transitions. In the NMR case we can combine Eqs. (14)–(16) and (19) of paper I to give

$$\rho(t_p) = 1 - \beta(\cos^2\tfrac{1}{2}\bar{\theta} + \sin^2\tfrac{1}{2}\bar{\theta}\cos 2\xi)\sum_i \sigma_{zi} - \beta(\sin^2\tfrac{1}{2}\bar{\theta}\sin 2\xi)\sum\sigma_{xi} - \beta(\sin\bar{\theta}\sin\xi)\sum\sigma_{yi}\,. \tag{23}$$

Neither 1 nor $\sum\sigma_{zi}$ generates single-quantum transitions, so they are unobservable. The only other two operators $\sum\sigma_{xi}$ and $\sum\sigma_{yi}$ are related by a phase shift, so the spectrum is independent of the flip angle except for an overall scale factor. In addition, it has long been known that the absorption spectrum is the Fourier transform of the free induction decay.[10]

In the optical case $\rho(t_p)$ is more complicated. The initial state $\Pi_i \sigma_{Gi} = \Pi_i 1_i - \sigma_{zi}$ is transformed by the relations in Eq. (14), paper I, to give:

$$\rho(t_p) = \prod_i [1_i - (\cos^2\tfrac{1}{2}\bar{\theta} + \sin^2\tfrac{1}{2}\bar{\theta}\cos 2\xi)\sigma_{zi} - (\sin^2\tfrac{1}{2}\bar{\theta}\sin 2\xi)\sigma_{xi} - (\sin\bar{\theta}\sin\xi)\sigma_{yi}]\,. \tag{24}$$

In the general case all 4^N N-site Pauli operators are produced. The equivalent expression in the single element basis is

$$\rho(t_p) = \prod_i [(\sin^2\tfrac{1}{2}\bar{\theta}\sin^2\xi)\sigma_{Ei} + (1-\sin^2\tfrac{1}{2}\bar{\theta}\sin^2\xi)\sigma_{Gi} + (-\sin^2\tfrac{1}{2}\bar{\theta}\sin 2\xi + i\sin\bar{\theta}\sin\xi)\sigma_i^+ + (-\sin^2\tfrac{1}{2}\bar{\theta}\sin 2\xi - i\sin\bar{\theta}\sin\xi)\sigma_i^-]\,. \tag{25}$$

If $\theta \ll 1$ or $\Delta\omega/\omega_1 \gg 1$ ($\xi \ll 1$, which corresponds to the weak pulse limit) then most of the molecules will remain in the ground state (the operator with the largest coefficient is $\Pi\sigma_{Gi}$ in this case), and the largest coherence will correspond to operators such as $\Pi_{j\neq1}\sigma_1^+\sigma_{Gj}$ which connect the total system ground state to a singly excited state. These transitions are of course the ones excited in classical optical spectroscopy with an incoherent source or low power laser.

The low power absorption spectrum $\chi''(\omega)$ can be derived through the theory of excitons.[4] We show in the Appendix that under certain conditions this spectrum is the Fourier transform of the free induction decay after an extremely small flip angle pulse, and as an aside that the moments[11] of the resonance curve are given by simple modifications to the NMR moment expansion outlined by Van Vleck.[5] We can thus compare experimental absorption spectra to the predicted free induction decays in this limit, as we shall discuss later.

B. Large flip angle spectra

For large pulse flip angles the spectrum changes. Such pulses give increased coefficients for many operators in Eq. (24) such as $\sigma_1^+\sigma_{E2}\Pi_{j>2}\sigma_{Gj}$ (transitions from singly to doubly excited states). This type of operator generates oscillating polarization, since its single nonzero matrix element is also a matrix element of σ_x

$=\sum\sigma_{xi}$. Therefore new transitions are observed, as has been noted previously for four-level systems.[12,13] Physically this difference between NMR and optical spectroscopy arises because the singly excited optical states are not populated at equilibrium, so weak irradiation will not induce transitions to higher states. In the high temperature approximation all states are populated at equilibrium, and weak irradiation can induce these transitions.

One important special case is $\theta=\pi$, $\xi=\pi/2$ (a π pulse on resonance), which gives

$$\rho(t_p)=\prod_i(\sigma_{Ei})\ . \tag{26}$$

All the molecules are transferred to the excited state and no coherences are produced. Another special case of interest is $\theta=\pi/2$, $\xi=\pi/2$ (a $\pi/2$ pulse on resonance), which gives

$$\rho(t_p)=\prod_i \tfrac{1}{2}(\sigma_{Ei}+\sigma_{Gi}+\sigma_i^+ +\sigma_i^-)\ . \tag{27}$$

Every matrix element of $\rho(t_p)$ in the localized excitation basis is equal to 2^{-N}. However, this does not mean that all transitions are equally strong, because the matrix elements will not be equal in the eigenbasis.

The exact spectrum can be calculated from Eqs. (19)–(22). Since N molecules produce a $2^N\times 2^N$ density matrix, this calculation is generally done by computer for all but very small systems. The calculations have been done for many NMR[6,7] systems and only the relative transition intensities change in optical spectroscopy. The four-level optical case is detailed in Refs. 12 and 13. As the number of coupled sites increases the number of observed NMR transitions increases rapidly, as shown in Fig. 3; the optical case is similar.

For large numbers of coupled sites the spectrum becomes an unresolvable "blob." The exact approach of calculating Eqs. (19)–(22) is not feasible because of the large number of eigenstates. However, the method of moments as developed for NMR[5,11] can be adapted[12] to give information on the optical line shape $F(\omega)$, here defined as the Fourier transform of the free induction decay (FID). Expressions for the second and fourth moments in the optical case were given in our earlier communication.[12] The Nth derivative of the FID at time $t=0$ is given by:

$$\langle\sigma_x(0)\rangle^N=\mathrm{Tr}\{i^N[\mathcal{H},[\mathcal{H}\cdots[\mathcal{H},\sigma_x]\cdots]]\rho_{eq}\}\ , \tag{28}$$
(N commutators)

$$\langle\sigma_y(0)\rangle^N=\mathrm{Tr}\{i^N[\mathcal{H},[\mathcal{H}\cdots[\mathcal{H},\sigma_y]\cdots]]\rho_{eq}\}\ . \tag{29}$$

The first few derivatives generate a polynomial in τ, which will not predict the behavior of the FID for long

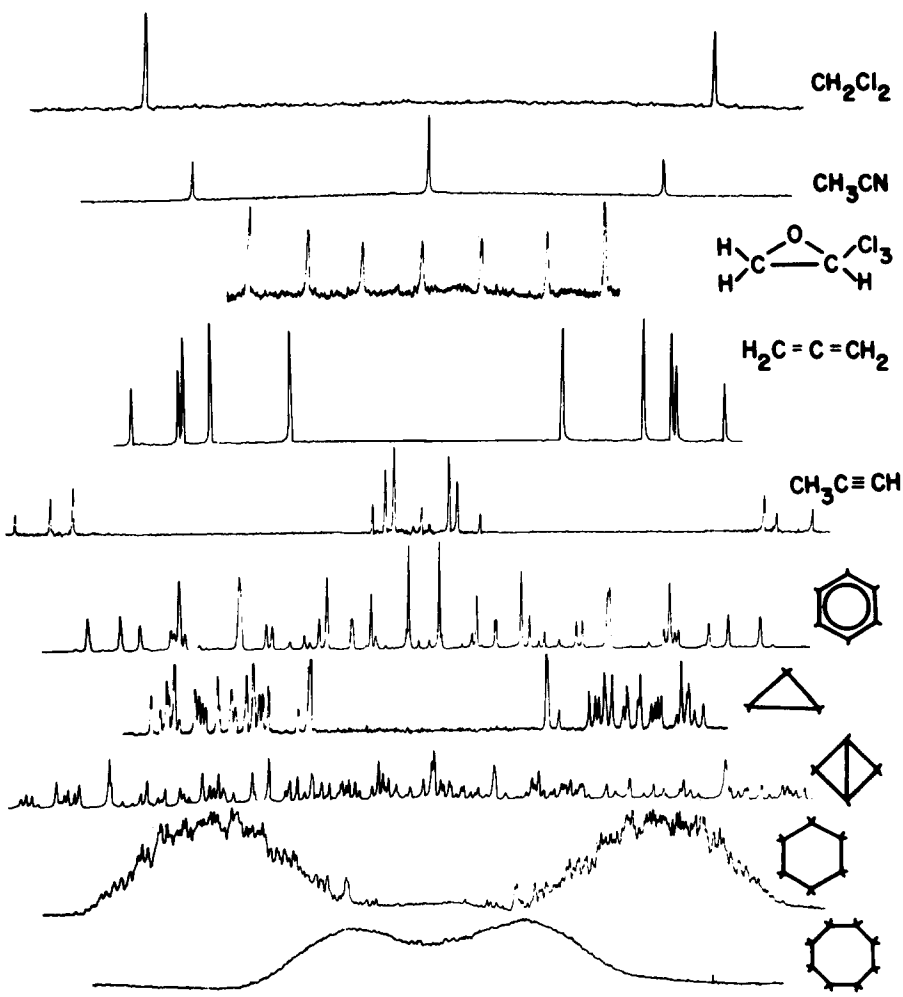

FIG. 3. NMR spectra of small molecules dissolved in liquid crystal solvents. Intramolecular couplings generate complicated energy level distributions, as illustrated in Figs. 1 and 2. As a result the spectral complexity increases dramatically as the number of coupled spins increases. As shown in Fig. 2, a similar though less dramatic increase would be expected for electronic transitions among N sites with analogous symmetries. Spectra courtesy of Dr. Z. Luz.

times. However, they may suggest a simple form (such as an exponential or Gaussian decay) which can be fit to the few known derivatives to give a lifetime. Another way of saying the same thing is to note that it is very difficult to get from the moments of $F(\omega)$ to its linewidth unless something is known about the line shape.[14] Fortunately there are good theoretical reasons for expecting a purely dipolar line shape to be roughly Lorentzian for a dilute mixed crystal.[15] Extending this argument to the V_{ij} terms of Eq. (11) gives simple expressions for the optical linewidth,[12] at least in the limit of an initial $\pi/2$ pulse on resonance. The expressions for the second and fourth moments are:

$$M_2 = \langle \omega^2 \rangle = \mathrm{Tr}\{[\mathcal{H}, [\mathcal{H}, \sigma_x]]\rho(t_p)\}/\mathrm{Tr}[\sigma_x \rho(t_p)] , \tag{30}$$

$$M_4 = \langle \omega^4 \rangle = \mathrm{Tr}\{[\mathcal{H}, [\mathcal{H}, [\mathcal{H}, [\mathcal{H}, \sigma_x]]]]\rho(t_p)\}/\mathrm{Tr}[\sigma_x \rho(t_p)] . \tag{31}$$

The moments from the V_{ij} terms alone in a crystal with fractional concentration f of guest molecules were shown to be

$$M_2 = f \sum_j V_{ij}^2 , \tag{32}$$

$$M_4 = 5f \sum_j V_{ij}^4 + 3f^2 \sum_{j \neq k} V_{ij}^2 V_{ik}^2 + 4f^2 \sum_{j \neq k} V_{ij}^2 V_{ik} V_{jk} . \tag{33}$$

These sums were evaluated for a cubic lattice and for an isotropic probability distribution and M_4/M_2^2 was shown to be large for $f \ll 1$. This suggested a Lorentzian line shape, which in the isotropic case was shown[12] to give a linewidth of

$$T_2^{-1} \sim 1.5 f \mu^2 a^{-3} \hbar^{-1} (f \ll 1) , \tag{34}$$

where μ is the transition dipole moment and a^{-3} is the unit cell volume. This zero-temperature dephasing will not be refocused by a conventional echo experiment, as we show in the next section.

C. Inhomogeneous broadening and echo experiments

Equation (34) assumes that the ω_i and Q_{ij} terms in the Hamiltonian of Eq. (11) can be neglected compared to the V_{ij} terms. It is not obvious that this is true, particularly in the light of our earlier discussion of the large inhomogeneous broadening in optical spectroscopy. Recent experimental measurements for pentacene in naphthalene[16] and naphthalene in durene[17] are consistent with transition multipole interactions contributing the dominant concentration dependent term to the coherence lifetime. However, there certainly are also optical density effects,[18] and the inhomogeneous broadening of 1 $\mathrm{cm}^{-1} = 30$ GHz is so much larger than the observed dephasing rate (~ 10 MHz for pentacene at a fractional concentration of 10^{-6}) that this broadening cannot be ignored.

For the moment let us assume the opposite limit, in which the $\sum \omega_i \sigma_{zi}$ terms dominate. The propagator $U = \exp(-i\mathcal{H}\tau)$ then has the form $\exp[i(A+B)]$, where

$$A = \sum \omega_i I_{zi} + \overline{\Delta\omega} I_z + \sum_{i,j} Q_{ij} \sigma_{zi} \sigma_{zi} ,$$

$$B = \sum_{i,j} V_{ij} (\sigma_{xi}\sigma_{xj} + \sigma_{yi}\sigma_{yj}) ,$$

and $\| A \| \gg \| B \|$. We can expand the propagator in terms of the small coefficients B_{ij}[19]:

$$\{\exp[i(A+B)]\}_{ij} = \exp(iA)_{ii}\delta_{ij} + B_{ij}\left[\frac{\exp(iA)_{ii} - \exp(iA)_{jj}}{A_{ii} - A_{jj}}\right] + \sum_k \frac{B_{ik}B_{kj}}{A_{jj} - A_{kk}}\left\{\frac{\exp(iA)_{ii} - \exp(iA)_{jj}}{A_{ii} - A_{jj}} - \frac{\exp(iA)_{kk} - \exp(iA)_{jj}}{A_{kk} - A_{jj}}\right\} + \cdots . \tag{35}$$

In Eq. (35) A is assumed to be diagonal in the ij basis set and B is assumed to be completely off-diagonal. This was the reason for putting the Q_{ij} terms in A; they are diagonal in the localized product basis set.

When τ is large the terms $\exp(iA)_{ii}$ are essentially random numbers of magnitude 1. The second term of Eq. (35) then shows that the B_{ij} terms will be unimportant if $|B_{ij}| \ll |A_{ii} - A_{jj}|$, which means $|V_{ij}| \ll |\omega_i - \omega_j|$. In NMR parlance this corresponds to the limit of first-order spectra. In that limit U becomes

$$U = \exp\left[-i\left(\Delta\omega_i \sigma_{zi} + \overline{\Delta\omega}\,\sigma_z + \sum_{i,j} Q_{ij}\sigma_{zi}\sigma_{zj}\right)\tau\right] = \exp[-i(\overline{\Delta\omega}\,\sigma_z\tau)] \exp\left(-i\sum_i \Delta\omega_i \sigma_{zi}\right) \times \exp\left(-i\sum_{i,j} Q_{ij}\sigma_{zi}\sigma_{zj}\tau\right) , \tag{36}$$

since all these terms are mutually commuting. The behavior is dominated by the inhomogeneous broadening, but the Q_{ij} terms are also quite important, as will be seen shortly.

If $|V_{ij}| \sim |\omega_i - \omega_j|$ then the expansion in Eq. (35) will converge only slowly or not at all and the transition dipolar couplings remain effective. The spatial distribution of the inhomogeneous broadening now determines whether or not dipolar interactions are important. For example, two dipoles with $\mu = 1$ D and a separation $r_{ij} = 100$ Å give $V_{ij} \sim \mu^2/r_{ij}^3 = 9.5 \times 10^8$ rad. If $\langle \omega_i^2 \rangle = 1$ $\mathrm{cm}^{-1} = 1.18 \times 10^{11}$ rad, and the resonance frequency of these two sites is uncorrelated, then this coupling can be ignored. On the other hand, if inhomogeneous broadening arises substantially from surface effects then molecules in the bulk of the material might be expected to have strongly correlated resonance frequencies, and this coupling (which is 1% of the inhomogeneous width)

may well be dominant. We will discuss experiments later which differentiate between these possibilities.

Photon echo sequences are typically used to study inhomogeneously broadened systems. We will consider here only the case $(\pi/2)_{-y} - \tau - (\pi)_y - \tau$ with ω_1 large; the phases were chosen for mathematical convenience. The transverse polarization $\langle\sigma_x\rangle$ after the second pulse is then

$$\begin{aligned}\langle\sigma_x\rangle = \mathrm{Tr}\{&\sigma_x \exp(-i\mathcal{H}\tau)\exp(-i\pi\sigma_y)\exp(-i\mathcal{H}\tau)\\ &\times\exp[+i(\pi/2)\sigma_y]\rho_{eq}\exp[-i(\pi/2)\sigma_y]\\ &\times\exp(i\mathcal{H}\tau)\exp(i\pi\sigma_y)\exp(i\mathcal{H}\tau)\}\ . \end{aligned}\tag{37}$$

Cyclic permutation of the operators, plus the relation $\sigma_x = \exp[-i(\pi/2)\sigma_y]\sigma_z\exp[i(\pi/2)\sigma_y]$, gives:

$$\begin{aligned}\langle\sigma_x\rangle = \mathrm{Tr}[&\rho_{eq}\exp(+i\mathcal{H}_x\tau)\exp(+i\mathcal{H}_{-x}\tau)\sigma_z\\ &\times\exp(-i\mathcal{H}_{-x}\tau)\exp(-i\mathcal{H}_x\tau)]\ , \end{aligned}\tag{38}$$

$$\mathcal{H}_x = \exp[-i(\pi/2)\sigma_y]\mathcal{H}\exp[+i(\pi/2)\sigma_y]$$

$$= \overline{\Delta\omega}\,\sigma_x + \sum_i \Delta\omega_i\sigma_{xi} + \sum_{i,j} Q_{ij}\sigma_{xi}\sigma_{xj} + \sum_{i,j} V_{ij}(\sigma_{zi}\sigma_{zj} + \sigma_{yi}\sigma_{yj})\ , \tag{39}$$

$$\begin{aligned}\mathcal{H}_{-x} &= \exp[i(\pi/2)\sigma_y]\mathcal{H}\exp[-i(\pi/2)\sigma_y]\\ &= -\overline{\Delta\omega}\,\sigma_x - \sum \Delta\omega_i\sigma_{xi} + \sum Q_{ij}\sigma_{xi}\sigma_{xj}\\ &\quad + \sum V_{ij}(\sigma_{zi}\sigma_{zj} + \sigma_{yi}\sigma_{yj})\ . \end{aligned}\tag{40}$$

A similar expression holds for $\langle\sigma_y\rangle$. The pulses have been made to rotate the operators of the Hamiltonian instead of the initial density matrix, which is an approach which will prove quite fruitful in the next section.

Equation (38) looks simpler than Eq. (37), but it still looks formidable. Fortunately it can be simplified further. The term $\overline{\Delta\omega}\,\sigma_x$ commutes with all other terms in $\mathcal{H}_x$ or $\mathcal{H}_{-x}$; it appears with opposite signs in $\mathcal{H}_x$ and $\mathcal{H}_{-x}$, so it cancels out:

$$\begin{aligned}U &= \exp(i\mathcal{H}_x\tau)\exp(i\mathcal{H}_{-x}\tau)\\ &= \exp\left\{i\tau\left[\sum_i \Delta\omega_i\sigma_{xi} + \sum_{i,j} Q_{ij}\sigma_{xi}\sigma_{xj} + \sum_{i,j} V_{ij}(\sigma_{zi}\sigma_{zj} + \sigma_{yi}\sigma_{yj})\right]\right\}\\ &\quad\times\exp(i\tau\overline{\Delta\omega}\,\sigma_x)\exp(-i\tau\overline{\Delta\omega}\,\sigma_x)\exp\left\{i\tau\left[-\sum_i \Delta\omega_i\sigma_{xi} + \sum_{i,j} Q_{ij}\sigma_{xi}\sigma_{xj} + \sum_{i,j} V_{ij}(\sigma_{zi}\sigma_{zj} + \sigma_{yi}\sigma_{yj})\right]\right\}\\ &= \exp\left\{i\tau\left[\sum_i \Delta\omega_i\sigma_{xi} + \sum_{i,j} Q_{ij}\sigma_{xi}\sigma_{xj} + \sum_{i,j} V_{ij}(\sigma_{zi}\sigma_{zj} + \sigma_{yi}\sigma_{yj})\right]\right\}\\ &\quad\times\exp\left\{i\tau\left[-\sum_i \Delta\omega_i\sigma_{xi} + \sum_{i,j} Q_{ij}\sigma_{xi}\sigma_{xj} + \sum_{i,j} V_{ij}(\sigma_{zi}\sigma_{zj} + \sigma_{yi}\sigma_{yj})\right]\right\}\ . \end{aligned}\tag{41}$$

If $Q_{ij} = V_{ij} = 0$ for all i and j then $U = 1$, meaning that the photon echo refocuses everything. If $|V_{ij}| \gg |Q_{ij}|$, $|\Delta\omega_i - \Delta\omega_j|$ then the off-diagonal terms dominate the line shape; if only the transition electric dipole–dipole interaction is included the photon echo decay will be the same as the FID is in the absence of inhomogeneities and the lifetime is given by Eq. (34).

Finally, if $|V_{ij}| \ll |\Delta\omega_i - \Delta\omega_j|$ then the V_{ij} terms can be neglected as before, and as before the Q_{ij} and $\Delta\omega_i$ terms are mutually commuting [Eq. (36)], so we are left with

$$U = \exp\left(2i\tau\sum_{i,j} Q_{ij}\sigma_{xi}\sigma_{xj}\right)\ . \tag{42}$$

Equation (42) then can be simplified further with the relations[20]

$$\begin{aligned}&\exp(-iQ_{ij}\sigma_{xi}\sigma_{xj}\tau)\sigma_{zi}\exp(iQ_{ij}\sigma_{xi}\sigma_{xj}\tau)\\ &\quad = \sigma_{zi}\cos(Q_{ij}\tau/2) - 2\sigma_{yi}\sigma_{xj}\sin(Q_{ij}\tau/2)\ , \end{aligned}\tag{43}$$

$$\begin{aligned}&\exp(-iQ_{ij}\sigma_{xi}\sigma_{xj}\tau)\sigma_{yi}\exp(iQ_{ij}\sigma_{xi}\sigma_{xj}\tau)\\ &\quad = \sigma_{yi}\cos(Q_{ij}\tau/2) + 2\sigma_{zi}\sigma_{xj}\sin(Q_{ij}\tau/2)\ . \end{aligned}\tag{44}$$

The exact coefficient of any desired operator in $U\sigma_z U^*$ can be obtained with a little algebraic manipulation. From Eq. (16) it is clear that ρ_{eq} contains no operators with σ_{xi} or σ_{yi} in them, so the only operators in both $U\sigma_z U^*$ and ρ_{eq} are the operators $\sigma_{zi}\Pi_j 1_j$. Therefore, Eq. (37) can be reduced to the simple expression

$$\langle\sigma_x\rangle \sim \sum_i \prod_j \cos(Q_{ij}\tau)\ . \tag{45}$$

In a small system the photon echo will be oscillatory, but in a real solid the sums run over a large enough number of sites N that the oscillations are probably unobservable. Equation (45) can be rewritten as the sum of $N2^{N-1}$ oscillating terms:

$$\langle\sigma_x\rangle \sim \sum \cos[(Q_{12} \pm Q_{13} \pm Q_{14} \cdots \pm Q_{1,N})\tau]\ , \tag{46}$$

where every possible arrangement of pluses and minuses appears exactly once in the sum. If all the Q_{ij} terms were roughly equal in magnitude then the distribution of frequencies would be roughly binomial, and a Gaussian decay would be observed. Instead $Q_{ij} \sim \mu^2/r_{ij}^3$, so that the line shape is less sharply peaked.

One way to visualize this decay is shown in Fig. 4. Figure 4(a) represents the crystal ground state, in which the resonance frequencies of all sites are affected equally by the coupling between permanent dipoles, although the frequencies will generally be different because of inhomogeneous broadening. When one molecule is excited its moments change, thus changing the resonance frequency of all its neighbors as in Fig. 4(b).

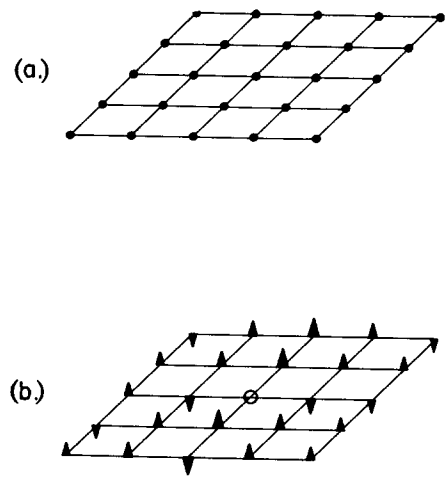

FIG. 4. Pictorial representation of photon echo decay through permanent multipole interactions in highly inhomogeneously broadened systems. Part (a) represents the crystal ground state, in which the resonance frequencies of all sites are affected equally by the coupling between permanent dipoles, although the frequencies will generally be different because of inhomogeneous broadening. When one molecule is excited its moments change, thus changing the resonance frequency of all its neighbors as in part (b). The inhomogeneous broadening is refocused by photon echoes, but the dipole–dipole interactions are bilinear and hence unaffected by the echo pulse, so they give the lifetime.

The inhomogeneous broadening is refocused by photon echoes, but these changes (corresponding to the Q_{ij} operators) are bilinear and hence unaffected by the echo pulse, so they give the lifetime.

It is straightforward to go from Eq. (46) to the moments of the resonance curve via a Taylor expansion:

$$M_{2N}=(-1)^N\left[d^{2N}\sigma_x(0)/dt^{2N}\right]/\sigma_x(0)\ , \tag{47}$$

$$M_2=\sum_j Q_{ij}^2\ , \tag{48}$$

$$M_4=\sum_j Q_{ij}^4+6\sum_{j>k} Q_{ij}^2 Q_{ik}^2\ . \tag{49}$$

Note that in the limit where all the Q_{ij} terms are equal this reduces to $M_4=[3-(2/N)]M_2^2$, which approaches a Gaussian as $N\to\infty$ as predicted earlier. In a dilute mixed crystal with fractional occupation probability $f\ll 1$ the formulas become

$$M_2=f\sum_j Q_{ij}^2\ , \tag{50}$$

$$M_4=f\sum_j Q_{ij}^4+6f^2\sum_{j>k} Q_{ij}^2 Q_{ik}^2\quad (f\ll 1)\ . \tag{51}$$

Calculations for an isotropic probability distribution or for dipoles aligned along the (100) direction of a cubic lattice follow the arguments of Refs. 11 and 12 exactly, so only the result will be given. For alignment in the (100) direction one finds

$$M_4=(2.38+0.21f^{-1})M_2^2\ , \tag{52}$$

so a pure crystal will be roughly Gaussian, and a dilute crystal is probably more Lorentzian. The dilute crystal ($f\ll 1$) dephasing time is

$$T_2^{-1}=1.25f\mu^2 a^{-3}\hbar^{-1}\ \text{[cubic lattice, (100) direction]}\ ,$$

$$T_2^{-1}=0.68f\mu^2 a^{-3}\hbar^{-1}\ \text{(isotropic distribution)}\ ,$$

with other dipole directions in the cubic lattice between these two values, and with μ defined as the change in the permanent dipole moment upon excitation.

We can summarize our photon echo results as follows.

(1) Inhomogeneous broadening will suppress any exchange or transition multipole interaction V_{ij} if $|V_{ij}|\ll|\Delta\omega_i-\Delta\omega_j|$. For long range broadening this simply means that an upper bound (which will correspond to many lattice spacings) should be put on the distance between interacting sites. This has very little effect on the sums in Eqs. (32)–(33) and hence does not really change the line shape.

(2) If the inhomogeneous broadening is short range then the permanent multipole interactions become the dominant factor in the photon echo line shape. This contribution will be particularly important if the permanent dipole moment changes substantially upon excitation, as in some molecular crystals.[21]

This calculation neglects optical density effects, which would generally produce coupling to Maxwell's equations in optically thick samples. These effects can be somewhat reduced by observing spontaneous emission, as discussed in paper I, and as was assumed here by writing $\langle\sigma_x\rangle$ as the observable instead of $\langle\sigma_x\rangle^2+\langle\sigma_y\rangle^2$. Nonlinear couplings of the sample polarization to the observable electric field are less important in this case.

Optical density effects can be entirely removed by observing optical multiple-quantum transitions, as discussed in the next section.

IV. EFFECTS OF MULTIPLE PULSE TRAINS IN MULTILEVEL SYSTEMS

A. Optical multiple-quantum spectroscopy

Equations (24) and (25) show that the density matrix produced by a single pulse on an optical system has operators such as $\sigma_1^+\sigma_2^+$, which generates two-quantum coherence, or $\sigma_1^+\sigma_2^-$, which generates coherence between two states which each have the same number of excited sites (zero-quantum coherences). These operators have some very interesting properties, which would make them useful for optical experiments. For example, the zero-quantum coherence is inherently free of long-range inhomogeneous broadening,[22] basically because as many photons go in as come out; if the absorbed photons are mismatched from resonance by $\overline{\Delta\omega}$ the emitted ones will be mismatched by the same amount, and the precession frequency of the coherence will not have a $\overline{\Delta\omega}$ term. In addition, neither of these operators corresponds to an oscillating polarization, since the polarization is proportional only to the single-quantum coherences $\sigma_x=\sum\sigma_{yi}$. Thus these operators are not coupled to Maxwell's equations and optical density effects are reduced.

Unfortunately, these operators are not directly observable, as noted in the discussion with Eqs. (19)–(22), precisely because they are not proportional to σ_x or σ_y.

Thus, some indirect detection scheme is needed. One well-known way around the identical problem is observing multiple-quantum NMR coherences is to use the pulse sequence in Fig. 5(a).[23–25] We will start by reviewing the NMR case, where $\rho_{eq} = 1 - \beta I_x$. The first two pulses (called the preparation sequence) are separated by a delay τ. At the end of the second pulse, the reduced density matrix is

$$\begin{aligned}\rho_{MQ}(t) &= 1 - \beta \exp(-i\pi I_y/2) \exp(-i\mathcal{H}\tau) \exp(i\pi I_y/2) I_x \exp(-i\pi I_y/2) \exp(i\mathcal{H}\tau) \exp(i\pi I_y/2) \\ &\equiv 1 - \beta \exp(-i\mathcal{H}_x\tau) I_x \exp(i\mathcal{H}_x\tau) \\ &\equiv 1 - \beta P(\tau) , \end{aligned} \tag{53}$$

$$\mathcal{H}_x = \sum_{i>j} D_{ij}(3I_{xi}I_{xj} - \mathbf{I}_i \cdot \mathbf{I}_j) + \sum_{i>j} J_{ij}(\mathbf{I}_i \cdot \mathbf{I}_j) - \sum \sigma_i I_{xi} + \Delta\omega I_x , \tag{54}$$

$\mathcal{H}_x$ as defined here is equivalent to Eq. (39). In general $\mathcal{H}_x$ will contain zero-quantum, one-quantum, and two-quantum operators, so the complex exponential can give ρ matrix elements corresponding to all multiple-quantum orders. After these pulses, the system evolves under $\mathcal{H}$ for a time t_1. Multiple-quantum NMR coherences do not correspond to oscillating magnetization, so a third pulse plus a delay t_2 are needed to partially transfer them back into the observables $\langle I_x \rangle$ and $\langle I_y \rangle$. The sequence is repeated with different values of t_1. The signal as a function of t_1 is

$$\begin{aligned}\langle M_x(t_1) \rangle &= C \operatorname{Tr}(\rho I_x) = C \operatorname{Tr}[\rho \exp(-i\pi I_y/2) I_x \exp(i\pi I_y/2)] \\ &= -C\beta \operatorname{Tr}[\exp(i\mathcal{H}_x t_2) I_x \exp(-i\mathcal{H}_x t_2) \exp(-i\mathcal{H}t_1) \exp(-i\mathcal{H}_x\tau) I_x \exp(i\mathcal{H}_x\tau) \exp(i\mathcal{H}t_1)] \\ &= -C\beta \sum_{ij} [P(\tau)]_{ji} [P(-t_2)]_{ij} \exp(i\omega_{ij}t_1) , \end{aligned} \tag{55}$$

where $P(-t_2)$ is defined by analogy with Eq. (53), and $\omega_{ij} = E_i - E_j$. The signal is Fourier transformed with respect to t_1 to produce a multiple-quantum spectrum. For simplicity of notation relaxation terms have been neglected; if $\tau_1, t_2 \ll T_2$ they can be included in Eq. (55) by replacing $\exp(i\omega_{ij}t_1)$ with $\exp(i\omega_{ij}t_1) \exp[-t_1/(T_2^*)_{ij}]$ (the inhomogeneous decay) when $i \neq j$, and $\exp[-t_1/(T_1)_{ii}]$, when $i = j$.

The only difference in the optical case is that the equilibrium density matrix has to be changed to correspond to Eq. (15). This gives

$$\sigma_x(t_1) = \sum_{i,j} Q(\tau)_{ji} P(-t_2)_{ij} \exp(i\omega_{ij}t_1) , \tag{56}$$

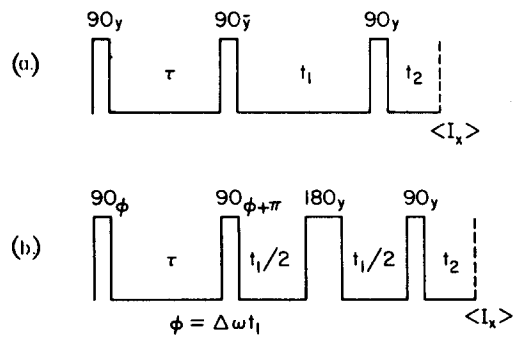

FIG. 5. NMR multiple-quantum pulse sequences. The optical analogs are derived by adding one more pulse and measuring fluorescence, as explained in the text. The sequence in part (a) generates a multiple-quantum spectrum when t_1 is varied, but the transitions are highly inhomogeneously broadened. The additional pulse in part (b) eliminates this broadening and the t_1-proportional incrementation of pulse phases measure the number of quanta in an individual transition (see the text).

$$Q(\tau) = \exp(-i\mathcal{H}_x\tau) \left(\prod \sigma_{Gi} \right) \exp(i\mathcal{H}_x\tau) . \tag{57}$$

In the optical case the delay τ and the second pulse are not needed to create multiple-quantum coherence, as shown in Eqs. (24) and (25). But the signal will be maximized by making $Q(\tau)$ and $P(-t_2)$ as similar as possible,[20] since

$$\sum_{ij} P_{ij}^2 = \operatorname{Tr}(P^2) = \operatorname{Tr}(\sigma_x^2) \quad \text{and} \quad \sum_{ij} Q_{ij}^2 = \operatorname{Tr}(Q^2) = \operatorname{Tr}(\rho_{eq}^2)$$

are constant. Since ρ_{eq} contains σ_x the two pulse preparation will probably enhance the optical signal.

Inspection of $\mathcal{H}$ shows that the n-quantum spectrum is centered at $n\overline{\Delta\omega}$ with the sequence in Fig. 5(a), so different values of n will be completely separated if $\overline{\Delta\omega}$ is greater than the spectral width $\|\mathcal{H}\|$. However, inhomogeneous broadening makes the n-quantum transitions n times wider than the single-quantum transitions. As a result, the multiple-quantum coherences will disappear very rapidly in an optical experiment. If $\langle \Delta\omega^2 \rangle^{1/2} = 1$ cm^{-1}, then all except zero-quantum coherences will disappear in a few picoseconds, even if the broadening is exclusively long range. Zero-quantum coherences will only be observable for $\tau, t_2 \gg D_{ij}^{-1}$, so the decay for small τ and t_2 will only have T_1 terms as was observed experimentally.[18]

The simplest way of removing this inhomogeneous broadening is to put echo pulses in t_1, as in Fig. 5(b). In this case the evolution propagator $\exp(-i\mathcal{H}t_1)$ is replaced with

$$\exp(-i\mathcal{H}t_1/2) \exp(i\pi I_y) \exp(-i\mathcal{H}t_1/2) , \tag{58}$$

which has the same properties as the photon echo evolution discussed in the last section. A multiple echo train, to be discussed in the next subsection, would be even

better.

Several different techniques exist for determining the number of quanta associated with a particular transition. A phase shift of ϕ in the first two pulses of any of the multiple-quantum sequences discussed so far will change $Q(\tau)$ in Eq. (57) to $Q'(\tau)$:

$$Q'(\tau) = \exp(-i\phi\sigma_x)\, Q(\tau) \exp(i\phi\sigma_x) , \tag{59}$$

$$Q'[(\tau)]_{ij} = [Q(\tau)]_{ij} \exp[-i\phi(m_i - m_j)] . \tag{60}$$

For example, if $\phi = \pi$ all of the $(2n+1)$-quantum coherence are multiplied by -1, but all the $(2n)$-quantum coherences are unaffected. Adding spectra with $\phi = 0$ to spectra with $\phi = \pi$ will eliminate all odd-quantum coherences.[22,24] This method is readily generalized; e.g., adding n spectra, each shifted by $\phi = 2\pi/n$, retains only transitions with $\Delta M = nk$ $(k = 0, \pm 1, \pm 2, \ldots)$.

A third method, which permits the simultaneous observation of all multiple-quantum transitions, is known as time proportional phase incrementation (TPPI).[24] In this experiment, whenever t_1 is incremented by Δt_1, the phases of the first two pulses are incremented by $\Delta\phi = (\Delta\omega')\Delta t_1$. Then $\phi = \Delta\omega' t_1$ in Eqs. (59) and (60). The n-quantum coherences appear to evolve at $n\Delta\omega' + \omega_{ij}$, so if $\Delta\omega' > \|\mathcal{H}\|$ all of the transitions are separated, and the spectrum is the same as would be produced by a homogeneous field without echoes.

The optical analog of selective excitation, a technique which dramatically enhances the high multiple-quantum spectra,[26] will be discussed elsewhere.[27]

B. Optical line narrowing sequences

1. Average Hamiltonian theory

The effect of any sequence of irradiating pulses and delays on a general system in the absence of relaxation can be represented by a single unitary transformation U (the propagator), as discussed in paper I. Calculating U directly by multiplying together the propagators for each part of the sequence is extremely tedious if many eigenstates are involved. However, this calculation can be avoided for certain pulse sequences (those which are called cyclic, defined below) by a technique known as average Hamiltonian theory. This technique is thoroughly documented,[28,29] so only a brief summary of important results will be reproduced here.

The total Hamiltonian of a system is written as $\mathcal{H}(t) = \mathcal{H}_{int} + \mathcal{H}_1(t)$, where $\mathcal{H}_{int}$ is the internal Hamiltonian of the system (e.g., the interactions V_{ij} and Q_{ij} between pairs of dipoles) and $\mathcal{H}_1(t)$ is the explicitly time-dependent interaction controlled by the experimenter (e.g., the interaction with radiation). $\mathcal{H}_1(t)$ is termed cyclic with cycle time t_c if $\mathcal{H}_1(t)$ and the propagator

$$U_1(t) = T \exp\left[-i \int_0^t \mathcal{H}_1(t')dt'\right]$$

are periodic (to within a sign),[28] and if t_c is the shortest interval that constitutes a period for both $U_1(t)$ and $\mathcal{H}_1(t)$. A pulse sequence which repeats itself is not automatically cyclic. For example, the photon echo sequence $(\frac{1}{2}T - \pi_x - \frac{1}{2}T)_N$ has an $\mathcal{H}_1$ which is periodic with repetition time T, but

$$U_1 = \exp(iN\pi\sigma_x) , \tag{61}$$

$$U_1(2t) = U_1(0) , \tag{62}$$

so U_1 is periodic with repetition time $2T$, and the cycle is two echoes [Fig. 6(a)]. If the pulses were not 180° the cycle time would be different; in fact U_1 might not be periodic at all.

If $\mathcal{H}_1(t)$ is a pulse sequence made up of an integral number N of cycles, the propagator for the entire sequence is the Nth power of the propagator corresponding to one cycle, and therefore only a single cycle need be considered. The propagator for a single cycle is the product of the propagators for each individual pulse or delay. Since each of the individual propagators is unitary, so is the product. The effects of the pulse sequence are assumed equivalent to what would be produced by some time independent "effective Hamiltonian" $\bar{\mathcal{H}}$. In fact, the propagator for a single cycle can be shown to be[28]:

$$U = \exp(-i\bar{\mathcal{H}}t_c) = \exp\{-i[\bar{\mathcal{H}}^{(0)} + \bar{\mathcal{H}}^{(1)} + \cdots + \bar{\mathcal{H}}^{(n)}]t_c\} , \tag{63}$$

where:

$$\bar{\mathcal{H}}^{(0)} = \frac{1}{t_c}\int_0^{t_c} \tilde{\mathcal{H}}_{int}(t)dt ,$$

$$\bar{\mathcal{H}}^{(1)} = \frac{-i}{2t_c}\int_0^{t_c} dt_2 \int_0^{t_2} dt_1 [\tilde{\mathcal{H}}_{int}(t_2), \tilde{\mathcal{H}}_{int}(t_1)] ,$$

$$\bar{\mathcal{H}}^{(2)} = -\frac{1}{6t_c}\int_0^{t_c} dt_3 \int_0^{t_3} dt_2 \int_0^{t_2} dt_1 \{[(\tilde{\mathcal{H}}_{int}(t_3), [\tilde{\mathcal{H}}_{int}(t_2), \tilde{\mathcal{H}}_{int}(t_1)]] + [\tilde{\mathcal{H}}_{int}(t_1), [\tilde{\mathcal{H}}_{int}(t_2), \tilde{\mathcal{H}}_{int}(t_3)]]\} \tag{64}$$

and

$$\tilde{\mathcal{H}}_{int}(t) = U_1^{-1}(t)\mathcal{H}_{int}U_1(t) . \tag{65}$$

This is a Magnus expansion of the propagator in powers of the cycle time.[29] It is equivalent to expanding the propagators of all the delays by Taylor series and grouping together terms with the same time dependence.

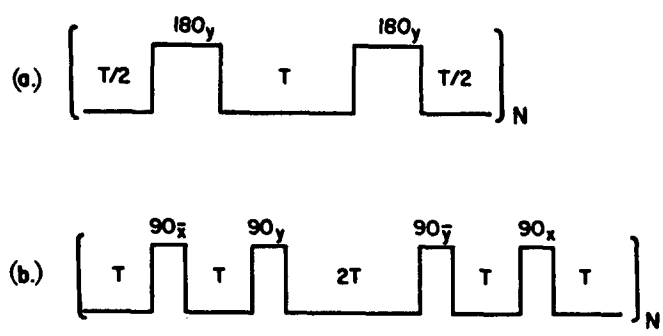

FIG. 6. Multiple-pulse sequences for suppressing some parts of the Hamiltonian. Part (a) shows a Carr–Purcell sequence, which eliminates inhomogeneous broadening to higher order than can be achieved with a simple photon echo. Part (b) shows a WAHUHA sequence, which eliminates second-rank tensor interactions such as dipole–dipole couplings. Theory and applications in optical spectroscopy are noted in the text.

The average Hamiltonian expansion is a perturbation expansion in powers of a smallness parameter t_c that has a physical meaning; t_c and $\tilde{\mathcal{H}}_{\rm int}(t)$ are simultaneously varied by lengthening the sequence. For this reason, $\bar{\mathcal{H}}^{(i)}$ is termed a correction term of order i and is proportional to t_c^i. $\bar{\mathcal{H}}^{(0)}$ is the zero-order or average Hamiltonian, and $\bar{\mathcal{H}}$ is the effective Hamiltonian.

2. Examples of multiple-pulse sequence

Pulse sequences are usually designed so that $\bar{\mathcal{H}}^{(0)}$ has some particular desired property and then higher-order terms are minimized. Two simple examples are shown in Fig. 6. Figure 6(a) is called a Carr–Purcell[30] sequence. We will assume that the pulses have negligible width, which is the high power limit. This gives

$$\begin{aligned}\tilde{\mathcal{H}}_{\rm int}(t) &= \overline{\Delta\omega}\,\sigma_x + \sum_i \Delta\omega_i\sigma_{zi} + \sum_{ij} J_{ij}(\sigma_i\cdot\sigma_j) + \sum_{ij} D_{ij}(3\sigma_{zi}\sigma_{zj} - \sigma_i\cdot\sigma_j)\ , \quad 0\le t\le T/2 \\ &= -\overline{\Delta\omega}\,\sigma_x - \sum_i \Delta\omega_i\sigma_{zi} + \sum_{ij} J_{ij}(\sigma_i\cdot\sigma_j) + \sum_{ij} D_{ij}(3\sigma_{zi}\sigma_{zj} - \sigma_i\cdot\sigma_j)\ , \quad T/2\le t\le 3T/2 \\ &= \overline{\Delta\omega}\,\sigma_x + \sum_i \Delta\omega_i\sigma_{zi} + \sum_{ij} J_{ij}(\sigma_i\cdot\sigma_j) + \sum_{ij} D_{ij}(3\sigma_{zi}\sigma_{zj} - \sigma_i\cdot\sigma_j)\ , \quad 3T/2\le t\le 2T\ . \end{aligned} \tag{66}$$

The first-rank tensors σ_{zi} are inverted by a 180° rotation. Zero-rank tensors $(\sigma_i\cdot\sigma_j)$ and second-rank tensors $(3\sigma_{zi}\sigma_{zj}-\sigma_i\cdot\sigma_j)$ are unaffected. Equation (64) then gives

$$\bar{\mathcal{H}}^{(0)} = \sum J_{ij}(\sigma_i\cdot\sigma_j) + \sum D_{ij}(3\sigma_{zi}\sigma_{zj} - \sigma_i\cdot\sigma_j) \tag{67}$$

and the inhomogeneous broadening has been exactly suppressed. Although it is not obvious from Eq. (64), if a pulse sequence is symmetric, such that $\tilde{\mathcal{H}}_{\rm int}(t) = \tilde{\mathcal{H}}_{\rm int}(t_c - t)$, $\bar{\mathcal{H}}^{(1)}$ and all other odd-order correction terms vanish.[28] This sequence is symmetric, so the major corrections come from $\bar{\mathcal{H}}^{(2)}$ and from pulse sequence imperfections (laser inhomogeneity, timing errors, and the like).

Figure 6(b) is called a WAHUHA[28] sequence. As before $\mathcal{H}$ can be decomposed into zero-rank, first-rank, and second-rank tensors. Zero-rank tensors (scalars) are unaffected by rotations, but this is not true for first-rank or second-rank tensors. For this sequence, $\tilde{\mathcal{H}}_{\rm int}$ is

$$\begin{aligned}\tilde{\mathcal{H}}_{\rm int}(t) &\sim (3\sigma_{zi}\sigma_{zj} - \sigma_i\cdot\sigma_j) + \sigma_{zi} + (\sigma_i\cdot\sigma_j) \quad (0\le t\le T) \\ &\sim (3\sigma_{yi}\sigma_{yj} - \sigma_i\cdot\sigma_j) + \sigma_{yi} + (\sigma_i\cdot\sigma_j) \quad (T\le t\le 2T) \\ &\sim (3\sigma_{xi}\sigma_{xj} - \sigma_i\cdot\sigma_j) + \sigma_{xi} + (\sigma_i\cdot\sigma_j) \quad (2T\le t\le 3T) \\ \tilde{\mathcal{H}}_{\rm int}(6T - t) &= \tilde{\mathcal{H}}_{\rm int}(t)\ . \end{aligned} \tag{68}$$

This gives

$$\begin{aligned}\bar{\mathcal{H}}^{(0)} &= \frac{1}{3}\Big[\overline{\Delta\omega}\,(\sigma_x+\sigma_y+\sigma_z) \\ &\quad + \sum_i \Delta\omega_i(\sigma_{xi}+\sigma_{yi}+\sigma_{zi})\Big] + \sum J_{ij}(\sigma_i\cdot\sigma_j) \\ \bar{\mathcal{H}}^{(1)} &= 0\ . \end{aligned} \tag{69}$$

This sequence eliminates dipolar terms and is used in NMR to observe chemical shifts in solids. More sophisticated sequences are designed to have smaller error terms. For example, one very powerful method of reducing these terms involving alternating between two or more different cycles (called subcycles) to form a new, larger cycle. Under certain conditions, some of the higher-order terms for the entire cycle are simply equal to the sum of the corresponding terms for the subcycles; such terms are said to decouple.[31] Decoupled pulse cycles for line narrowing have been produced that have $\bar{\mathcal{H}}^{(2)} = 0$ for the dipolar Hamiltonian and have small error terms.[31]

Physically, the dipolar interaction can be refocused because it vanishes when averaged over all of space, or over three orthogonal coordinate axes. This average

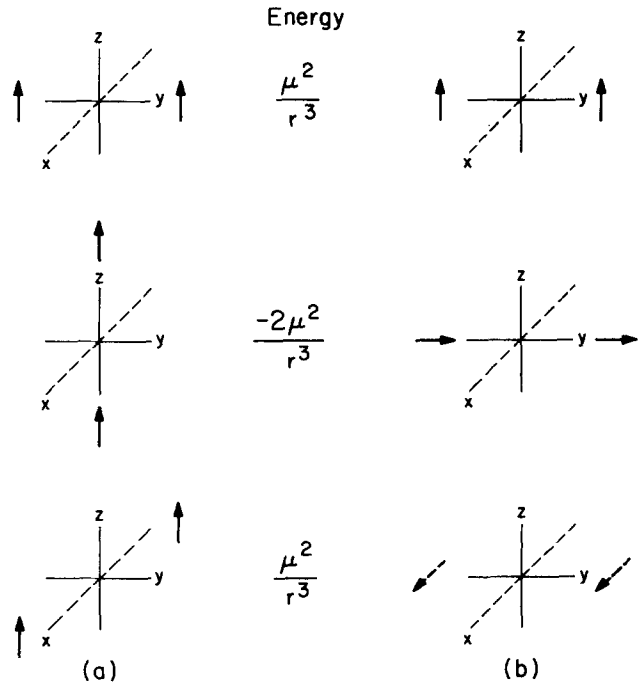

FIG. 7. Schematic illustration of how sample rotation in NMR [part (a)] or multiple-pulse sequences in NMR or optics [part (b)] can make second-rank tensor interactions such as dipole–dipole couplings vanish. The interaction energies change as the sites of the dipoles are rotated. If the rotations are done rapidly compared to relaxation times or other line broadening rates only the average interaction survives.

can either be done spatially (in NMR by rotating the sample), as in Fig. 7(a), or in spin space (in NMR or optical spectroscopy), as in Fig. 7(b).

3. Estimation of correction terms

Higher-order terms are usually difficult to calculate, but their size (and therefore their contribution to residual linewidths) can sometimes be estimated. If $\bar{\mathcal{H}}^{(0)} = \bar{\mathcal{H}}^{(1)} = \bar{\mathcal{H}}^{(2)} \cdots \bar{\mathcal{H}}^{(n-1)} = 0$, then $\bar{\mathcal{H}}^{(k)} = \bar{\bar{\mathcal{H}}}^{(k)}$, where $\bar{\bar{\mathcal{H}}}^{(k)}$ is defined as[26,28]

$$\bar{\bar{\mathcal{H}}}^{(k)} = \frac{(-i)^k}{t_c} \int_0^{t_c} dt_{k+1} \int^{t_{k+1}} dt_k \cdots \int_0^{t_2} dt_1 \times \bar{\mathcal{H}}_{\rm int}(t_{k+1}) \bar{\mathcal{H}}_{\rm int}(t_k) \cdots \bar{\mathcal{H}}_{\rm int}(t_1); \; n \leq k \leq 2n. \tag{70}$$

The implications for optical spectroscopy are as follows:

(1) $\bar{\mathcal{H}}^{(2)}$ for a Carr–Purcell sequence will be negligible if $|\Delta\omega_i t_c| \ll 1$ for all sites. This implies that a very short delay between pulses should be used. In that limit, the D_{ij} and J_{ij} terms (or, equivalently, the Q_{ij} and V_{ij} terms) generate the observed decay. The suppression of V_{ij} by $\Delta\omega_i - \Delta\omega_j$, as discussed in conjunction with Eq. (41), does not occur; all the dipoles interact as if they were perfectly resonant.

Other multiple echo sequences, discussed in Ref. 28, will better compensate for laser inhomogeneities and finite pulse widths.

(2) The D_{ij} couplings are eliminated by a WAHUHA sequence, but J_{ij} couplings are unaffected. This does not directly eliminate transition electric dipole interactions, because $J_{ij} = \frac{1}{3}(Q_{ij} + 4V_{ij})$. However, if the inhomogeneities $\Delta\omega_i$ are also eliminated, then the J_{ij} couplings are unobservable. This can be seen by writing down the time evolution of $\langle\sigma_x\rangle$ or $\langle\sigma_y\rangle$ [Eqs. (19)–(22)] under those couplings alone:

$$\begin{aligned}\langle\sigma_x(\tau)\rangle &= \mathrm{Tr}\left[\sigma_x \exp\left(-i\tau \sum_{i,j} J_{ij}\sigma_i\sigma_j\right)\rho(t_p)\exp\left(+i\tau\sum J_{ij}\sigma_i\sigma_j\right)\right] \\ &= \mathrm{Tr}\left[\exp\left(i\tau\sum_{ij} J_{ij}\sigma_i\cdot\sigma_j\right)\sigma_x \exp\left(-i\tau\sum_{ij} J_{ij}\sigma_i\cdot\sigma_j\right)\rho(t_p)\right] \\ &= \mathrm{Tr}[\sigma_x\rho(t_p)] = \langle\sigma_x(0)\rangle \end{aligned} \tag{71}$$

because $[\sigma_i \cdot \sigma_j, \sigma_x] = 0$. Sequences which remove both D_{ij} and $\Delta\omega_i$ can be readily designed. One conceptually simple way to do this is to replace each interval T of the WAHUHA sequence in Fig. 6(b) with the Carr–Purcell sequence of Fig. 6(a). The response of the system to this combined sequence will reflect only true relaxation effects such as fluctuations.

V. APPLICATIONS TO MIXED CRYSTALS AND EXCITONS

A. Absorption spectra

In particularly simple cases the Hamiltonian of Eq. (12) can be diagonalized to give the exact absorption line shape. Consider, e.g., the electronic absorption line shape of 1, 4-dibromonaphthalene (DBN) crystal,[32–35] which is shown in Fig. 8(a). The line shape is asymmetric, looking roughly like a Lorentzian on the high energy side and cutting off sharply with decreasing excitation energy. The crystal structure shows two molecules in a subunit cell which is very short in one direction. In this direction each molecule has a large pi-electron overlap with its two nearest neighbors, giving a large exchange coupling ($V_{i,i\pm1} = -6.2$ cm^{-1}) in that direction but virtually no coupling in any other direction. Thus, the crystal looks mathematically like a one-dimensional structure. In a long chain of equivalent sites only the totally symmetrical state is accessible from the ground state, so the observed line shape must come from some term in the Hamiltonian which breaks the equivalence, such as inhomogeneous broadening.

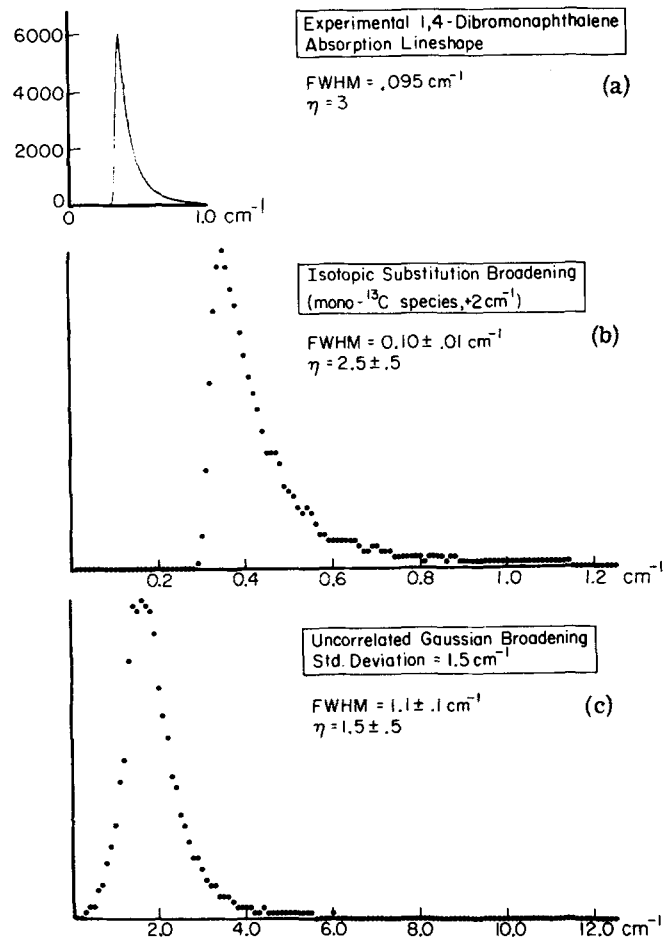

FIG. 8. Simulated and observed spectra for the low temperature absorption of 1,4-dibromonaphthalene (DBN). The experimental spectrum [part (a)] is quite sharp (FWHM = 0.095 cm^{-1}) and asymmetric (η = upper half-width/lower half-width = 3). Monte Carlo line shape simulations were generated for exchange couplings combined with natural abundance ^{13}C substitution [part (b)] or an uncorrelated Gaussian distribution of site energies [part (c)]. While earlier approximate Green's function calculations in Refs. 32 and 33 gave qualitative agreement for both of these models with experiment, our calculations show that only the isotopic substitution model is tenable. (Experimental figure courtesy of H. Port, see Ref. 35.)

The Green's function formalism has been used to predict the effects of different postulated inhomogeneous distributions on the line shape.[32,33] For example, mono-^{13}C species are naturally present in 1% abundance

at each of the ten carbons. This isotopic substitution tends to shift the resonance frequency[34] by about 2 cm^{-1} and this distribution (i.e., 10% probability of $\Delta\omega_i = 2$ cm^{-1}) was used with the coherent potential approximation in Ref. 32 to predict a qualitatively correct line shape.

On the other hand, in Ref. 33 the molecular resonance frequencies were assumed uncorrelated and given by a Gaussian distribution. The average t-matrix approximation to the Green's function was shown to give qualitative agreement with experiment when $\langle\Delta\omega^2\rangle^{1/2} = 1.5$ cm^{-1}. Several other models for the DBN line shape have also been proposed.

As a first step towards resolving this question, we tested these approximations by generating a set of resonance frequencies for the sites of a 100-molecule chain according to each of these postulated distributions, diagonalizing the Hamiltonian, and calculating the spectrum from Eq. (20). We then averaged over many distributions. Our results agree with the Green's function calculation in the isotopic substitution case, with our fit to experimental data being somewhat better [Fig. 8(b)]. On the other hand, our calculated line shape for the Gaussian distribution of Ref. 33 does not agree with their calculations or with experiment [Fig. 8(c)]. This may suggest that the average t-matrix approximation is less adequate for DBN. Multiple pulse trains, including multiple echoes and dipolar narrowing sequences in particular, will be very useful in more thoroughly resolving these questions.

B. Dephasing

Photon echo line shapes in molecular crystals can be explained by many different mechanisms, as shown by several recent papers[12,13,16–18] and by our results in Sec. III C. Experiments with varying concentrations and thicknesses have eliminated some of these mechanisms but are not likely to be conclusive, since macroscopic crystals begin to grow optically dense at the same concentrations where multipole interactions become important.

On the other hand, the responses of molecular crystals to different multiple-pulse sequences will be quite informative, as we have shown. A purely dipolar dephasing[12] can be refocused by a WAHUHA sequence. A dephasing from Q_{ij} terms as discussed in Sec. III C can only be refocused by a sequence which also eliminates inhomogeneous effects, as discussed in Sec. IV B. Finally, optical density effects[18] can be substantially eliminated by multiple-quantum sequences.

Apart from these qualitative differences, multiple-pulse sequences also make quantitative measurements of interaction strengths possible, since the reciprocal of the time delay between pulses sets the approximate maximum interaction strength (converted to frequency units) which can be refocused. In moderate sized systems exact calculations of the propagator for even complex pulse sequences are possible.[36] Thus, observed multiple-pulse spectra can be used to determine couplings.

VI. CONCLUSIONS

Optical multilevel systems can be quite generally understood by the density matrix and average Hamiltonian formalisms developed for nuclear magnetic resonance. For simplicity we have restricted ourselves to the strong pulse limit to show the principles of the calculations, but generalizations are currently in progress. We have demonstrated the effects of permanent and transition multipole interactions, exchange couplings, inhomogeneous broadening, and lattice perturbations on absorption line shapes, single pulse experiments, and echo experiments. We have also discussed the applicability of the two new techniques of optical multiple-quantum spectroscopy and optical line narrowing to extract new information in low temperature solids. We expect that many future experiments will use these techniques.

ACKNOWLEDGMENTS

This work was supported by a grant from the National Science Foundation, No. DMR81-05034. We wish to thank Dr. Zeev Luz for permission to use his spectra in Fig. 3, and Dr. H. Port for permission to use their spectrum of 1, 4-dibromonaphthalene in Fig. 8(a) prior to publication.

APPENDIX: DERIVATION OF MOMENTS FOR ABSORPTION LINE SHAPE

We start from the Kramers–Kronig relations and the derivation for NMR contained in Abragam,[10] p. 100–101, up to his Eq. (10):

$$\chi''(\omega) = \frac{-iV}{\hbar}\int_0^\infty \sin(\omega t')\,\mathrm{Tr}([\rho_0, e^{-i\mathcal{H}t'}\sigma_x e^{i\mathcal{H}t}]\sigma_x)dt' , \quad \text{(A1)}$$

where V is the sample volume, and ρ_0 is the equilibrium density matrix. At this point the optical and NMR derivations will differ. In optics $\rho_0 = \Pi_i \sigma_{Gi}$, so we have:

$$\chi''(\omega) = \frac{+iV}{\hbar}\int_0^\infty \sin(\omega t')\,\mathrm{Tr}(e^{+i\mathcal{H}t'}\sigma_x e^{-i\mathcal{H}t'}[\rho_0, \sigma_x])dt'$$
$$= \frac{V}{\hbar}\int_0^\infty \sin(\omega t')\left\{\mathrm{Tr}\left[e^{+i\mathcal{H}t'}\sigma_x e^{-i\mathcal{H}t'}\left(\prod_i I_{yi} I_{Gj}\right)\right]\right\}dt . \quad \text{(A2)}$$

This implies that $\chi''(\omega)$ is the Fourier transform of the small flip angle FID (the term in brackets). Thus, the absorption line shape, to the extent that it reflects $\chi''(\omega)$ and the distribution of eigenstates, can be determined from pulse measurements.

Define

$$\sigma_x(t) = e^{+i\mathcal{H}t}\sigma_x e^{-i\mathcal{H}t} ; \quad G'(t) = \mathrm{Tr}\left[\sigma_x(t)\left(\prod_i I_{yi} I_{Gj}\right)\right]$$

$$G'(t) = \mathrm{Tr}\left[e^{+i\mathcal{H}t}\sigma_x e^{-i\mathcal{H}t}\left(\prod_i \sigma_{yi}\sigma_{Gj}\right)\right]$$

$$= \mathrm{Tr}\left[\exp(i\omega_0\sigma_x t)\exp(i\mathcal{H}_1' t)\,\sigma_x \exp(-i\mathcal{H}_1' t)\right.$$
$$\left.\times \exp(-i\omega_0\sigma_x t)\left(\prod_i \sigma_{yi}\sigma_{Gj}\right)\right] , \quad \text{(A3)}$$

$$= \cos\omega_0 t \left\{ \mathrm{Tr}\left[\exp(i\mathcal{H}_1' t)\sigma_x \exp(-i\mathcal{H}_1 t)\left(\prod_i \sigma_{yi}\sigma_{Gj}\right)\right]\right\}$$

$$- \sin\omega_0 t \left\{ \mathrm{Tr}\left[\exp(i\mathcal{H}_1' t)\sigma_x \exp(-i\mathcal{H}_1 t)\left(\prod_i \sigma_{xi}\sigma_{Gj}\right)\right]\right\}$$

$$\equiv G_c(t)\cos\omega_0 t + G_s(t)\sin\omega_0 t \ . \tag{A4}$$

Writing $h(u) = F(\omega_0 + u)$ gives

$$h(u) = A\int_{-\omega_0}^{\infty} \sin(u+\omega_0) G'(t)\,dt \tag{A5}$$

$$G'(t) = \frac{2}{\pi A}\int_{-\omega_0}^{\infty} h(u)\sin(\omega_0+u)t\,du$$

$$= \frac{2}{\pi A}\left\{ \int h(u)\sin\omega_0 t\cos ut\,du + \int h(u)\cos\omega_0 t\sin ut\,du\right\} . \tag{A6}$$

Extending the lower limit to $-\infty$, which is valid for transitions with small fractional linewidths, gives

$$G_c(t) = \frac{2}{\pi A}\int_{-\infty}^{\infty} h(u)\sin ut\,du \ , \tag{A7}$$

$$G_s(t) = \frac{2}{\pi A}\int_{-\infty}^{\infty} h(u)\cos ut\,du \ . \tag{A8}$$

Now the nth moment M_n is given by

$$M_n = \int_{-\infty}^{\infty} u^n h(u)\,du \Big/ \int_{-\infty}^{\infty} h(u)\,du$$

$$= (-1)^{n-1}\left(\frac{d^n G_c(t)}{dt^n}\right)_{t=0} / G_s(0) \quad (n \text{ odd}) \ , \tag{A9}$$

$$= (-1)^n \left(\frac{d^n G_s(t)}{dt^n}\right)_{t=0} / G_s(0) \quad (n \text{ even}) \ , \tag{A10}$$

and since

$$\frac{d^p G_c(t)}{dt^p} = (i)^p \,\mathrm{Tr}([\mathcal{H}_1', [\mathcal{H}_1' \cdots [\mathcal{H}_1', \sigma_x]]]\cdots]\{I_{xi} I_{Gj}\}) \ , \tag{A11}$$

[a similar formula holds for $G_s(t)$]

$$G_s(0)M_{2n+1} = \mathrm{Tr}(\underbrace{-i[\mathcal{H}_1', [\mathcal{H}_1' \cdots, [\mathcal{H}_1', I_y]]]\cdots}_{2n+1 \text{ times}}\{I_{xi} I_{Gj}\}) \ , \tag{A12}$$

$$G_s(0)M_{2n} = \mathrm{Tr}([\mathcal{H}_1', \cdots [\mathcal{H}_1', I_y]]]\cdots]\{I_{yi} I_{Gj}\}) \ . \tag{A13}$$

[1] W. R. Lambert, P. M. Felker, and A. H. Zewail, J. Chem. Phys. 75, 5958 (1981); A. Zewail, W. Lambert, P. Felker, J. Perry, and W. Warren, J. Phys. Chem. 86, 1184 (1982).
[2] W. R. Lambert, P. M. Felker, and A. H. Zewail, Chem. Phys. Lett. 89, 309 (1982).
[3] J. Chaiken, M. Gurnick, and J. D. MacDonald, J. Chem. Phys. 74, 106 (1981); E. Schlag (private communication); S. Okajima, H. Saigusa, and E. C. Lim. J. Chem. Phys. 76, 2096 (1982).
[4] A. S. Davydov, *Theory of Molecular Excitons* (Plenum, New York, 1971).
[5] J. H. Van Vleck, Phys. Rev. 74, 1168 (1948).
[6] J. W. Emsley and J. C. Lindon, NMR *Spectroscopy Using Liquid Crystal Solvents* (Pergamon, Oxford, 1975).
[8] W. S. Warren and A. H. Zewail, J. Chem. Phys. 78, 2279 (1983).
[9] A. Saupe, Z. Naturforsch. Teil A 19, 161 (1964).
[10] A. Abragam, *The Principles of Nuclear Magnetism* (Oxford, London, 1961).
[11] C. Kittel and E. Abrahams, Phys. Rev. 20, 238 (1953).
[12] W. S. Warren and A. H. Zewail, J. Phys. Chem. 85, 2309 (1981).
[13] J. L. Skinner, H. C. Andersen, and M. D. Fayer, J. Chem. Phys. 75, 3195 (1981); R. W. Olson, F. G. Patterson, H. W. H. Lee, and M. D. Fayer, Chem. Phys. Lett. 77, 403 (1981).
[14] W. J. C. Grant, Physica (Utrecht) 30, 1433 (1964).
[15] P. W. Anderson, Phys. Rev. 82, 342 (1951).
[16] D. E. Cooper, R. W. Olson, and M. D. Fayer, J. Chem. Phys. 72, 2332 (1980).
[17] J. B. W. Morsink, B. Kruizinga, and D. A. Wiersma, Chem. Phys. Lett. 76, 218 (1980).
[18] R. W. Olson, H. W. H. Lee, F. G. Patterson, and M. D. Fayer, J. Chem. Phys. 76, 31 (1982).
[19] P. L. Corio, *Structure of High-Resolution* NMR *Spectra* (Academic, New York, 1966).
[20] W. S. Warren, Ph.D. thesis, University of California, Berkeley, 1979 (published as Lawrence Berkeley Laboratory Report No. 11885). J. B. Murdoch, W. S. Warren, D. P. Weitekamp, and A. Pines, J. Magn. Reson. (submitted).
[21] R. H. Young and A. P. Marchetti (private communication).
[22] A. Wokaun and R. R. Ernst, Mol. Phys. 36, 317 (1978).
[23] M. E. Stoll, A. J. Vega, and R. W. Vaughan, J. Chem. Phys. 67, 2029 (1977).
[24] S. Vega, T. W. Shattuck, and A. Pines, Phys. Rev. Lett. 37, 43 (1976); G. Drobny, A. Pines, S. Sinton, D. P. Weitekamp, and D. Wemmer, Faraday Symp. Chem. Soc. 13, 49 (1979).
[25] G. Bodenhausen, R. L. Vold, and R. R. Vold, J. Magn. Reson. 37, 93 (1980); A. Wokaun and R. R. Ernst, Chem. Phys. Lett. 52, 407 (1977); H. Hatanaka, T. Terao, and T. Hashi, J. Phys. Soc. Jpn. 39, 835 (1975).
[26] W. S. Warren, S. Sinton, D. P. Weitekamp, and A. Pines, Phys. Rev. Lett. 43, 1791 (1979); W. S. Warren, D. P. Weitekamp, and A. Pines, J. Chem. Phys. 73, 2084 (1980); W. S. Warren and A. Pines, *ibid.* 74, 2808 (1981).
[27] W. S. Warren and A. H. Zewail, J. Chem. Phys. (Flygare issue).
[28] J. S. Waugh, L. M. Huber, and U. Haeberlen, Phys. Rev. Lett. 20, 180 (1968); U. Haeberlen and J. S. Waugh, Phys. Rev. 175, 453 (1968); U. Haeberlen, *Advances in Magnetic Resonance* (Academic, New York, 1976), Suppl. 1.
[29] W. Magnus, Commun. Pure Appl. Math. 1, 649 (1954).
[30] H. Y. Carr and E. M. Purcell, Phys. Rev. 94, 630 (1954).
[31] D. P. Burum and W-K. Rhim, J. Chem. Phys. 71, 944 (1979).
[32] D. M. Burland, J. Chem. Phys. 59, 4383 (1973); D. M. Burland and R. M. MacFarlane, J. Lumin. 12–13, 213 (1976); D. M. Burland, U. Konzelmann, and R. M. MacFarlane, J. Chem. Phys. 67, 1926 (1977); R. M. Macfarlane, U. Konzelmann, and D. M. Burland, *ibid.* 65, 1022 (1976).
[33] J. Klafter and J. Jortner, J. Chem. Phys. 68, 1513 (1978).
[34] For a recent review see D. Burland and A. H. Zewail, Adv. Chem. Phys. 40, 369 (1979).
[35] H. Port, University of Stuttgart (unpublished).
[36] W. S. Warren, J. B. Murdoch, and A. Pines, J. Magn. Reson. (in press).